Turbo-Decoding of a convolutionally encoded OCDMA System

Daniel Efinger and Robert Fritsch
Institute of Telecommunications, University of Stuttgart,
Pfaffenwaldring 47, 70569 Stuttgart, Germany
{efinger,fritsch}@inue.uni-stuttgart.de

ABSTRACT

We present a novel multiple access scheme for Passive Optical Networks (PON) based on optical Code Division Multiple Access (OCDMA). Different from existing proposals for implementing OCDMA, we replaced the predominating orthogonal or weakly correlated signature codes (e.g. Walsh-Hadamard codes (WHC)) by convolutional codes. Thus CDMA user separation and forward error correction (FEC) are combined. The transmission of the coded bits over the multiple access fiber is carried through optical BPSK. This requires electrical field strength detection rather than direct detection (DD) at the receiver end. Since orthogonality gets lost, we have to employ a multiuser receiver to overcome the inherently strong correlation. Computational complexity of multiuser detection is the major challenge and we show how complexity can be reduced by applying the turbo principle known from soft-decoding of concatenated codes. The convergence behavior of the iterative multiuser receiver is investigated by means of extrinsic information transfer charts (EXIT-chart). Finally, we present simulation results of bit error ratio (BER) vs. signal-to-noise ratio (SNR) including a standard single mode fiber in order to demonstrate the superior performance of the proposed scheme compared to those using orthogonal spreading techniques.

Keywords: Optical Code Division Multiple Access (OCDMA), multiuser detection, soft-in/soft-out decoding, iterative demapping and decoding, EXIT-chart

1. INTRODUCTION

Optical Code Division Multiple Access (OCDMA) is an alternative multiplexing scheme to the more conventional Wavelength Division Multiple Access (WDMA) and Time Division Multiple Access (TDMA). The advantages OCDMA offers, e.g. in the upstream direction of a Passive Optical Network (PON) (cf. Fig. 1), may be identified in terms of network granularity and the flexibility in the management of the system resources.

Implementation of OCDMA with direct sequence spreading is associated with the request for appropriate signature code design. Rendering the signature codes orthogonal or even allowing a small amount of correlation has been the leading design principle so far since it allows for simple receiver structures. Famous representatives

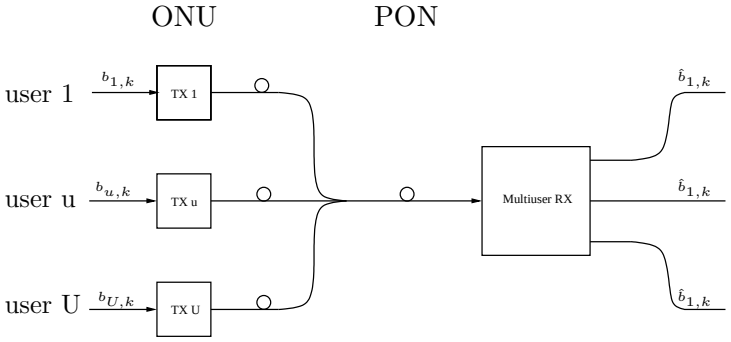

Figure 1. Upstream direction in a PON.

are optical orthogonal codes[1–3] or Walsh-Hadamard codes (WHC). Nevertheless, a system with perfect synchronization among the users is very costly and difficult to implement and OTDMA is then a concurrent alternative to synchronous OCDMA. Furthermore, the implementation of orthogonal spreading techniques in fiber-based networks with direct detection (DD) has to face further constraints compared to wireless CDMA applications for example. Thus for unipolar encoding there will always be some correlation among signature codes present which cancels the effect of orthogonal signature design and therefore has to be compensated by multiuser (MU) detection.

In general, it is possible to take any type of code for spreading purposes as long as correlation is taken into account in a possibly required MU-receiver. In this paper we replaced the conventional signature codes by convolutional codes which normally show strong correlation because the output codeword is computed by means of linear shift registers using modulo-2 arithmetic. Consequently, applying MU-detection is inevitable. On the other hand, the interpretation of the received samples as output of a noisy Markovian source leads us to efficient trellis based decoding algorithms which are able to deal with MU-interference as well as receiver noise. This approach combines MU-detection and forward error correction (FEC). It remains to find a structure of the MU-receiver which has reasonable computational complexity. A first straightforward realization is given by joint Viterbi decoding[4,5] which is based on a common trellis derived from the different parameters of the convolutional codes of active users. However, the number of states and transitions in the common trellis depends exponentially on the number of users which makes this approach not feasable even for moderate numbers of users. Hence, we will precisely investigate the components of a convolutionally encoded OCDMA system in Section 2 and derive a reduced complexity iterative MU-receiver. This MU-receiver applies turbo-like processing known from decoding of concatenated codes used for efficient channel coding. Subsequently, Section 3 gives a condensed mathematical insight in the iterative MU-detection algorithm. This is followed in Section 4 by performance evaluations of the iterative receiver in presence of additive noise (AWGN) generated by the coherent demodulation device. The use of extrinsic information transfer charts (EXIT-chart) is a major means for this purpose. In Section 5 a standard single mode fiber suffering from chromatic as well as polarization mode dispersion and fiber non-linearities is included in the system model and simulation results are presented. Finally, we conclude and specify possible future work.

2. SYSTEM MODEL

2.1. Optical Networking Unit (TX)

In Fig. 2 a) we present the principle structure of a user's optical networking unit (ONU) for convolutionally encoded OCDMA. The information bits are denoted by $b_{u,k}$ where $u \in \{1, \ldots, U\}$ represents the user index and $k \in \mathbb{Z}$ is the discrete-time index. The respective bit rate is given by $1/T_b$. We use recursive convolutional codes (RSC) as signature codes. Thus spreading is performed by use of a recursive convolutional encoder which outputs the coded bits $c_{u,m}$ at a rate of $1/T_c = L/T_b$. The spreading factor L refers directly to the code rate R_c

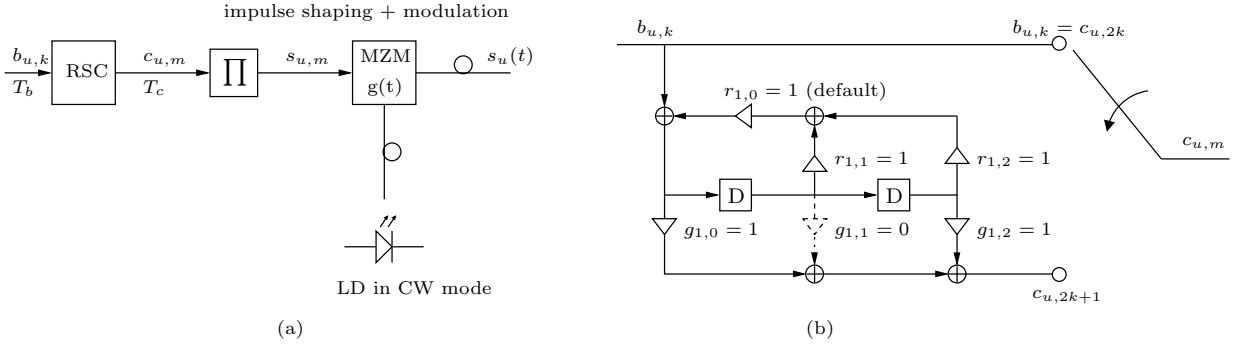

Figure 2. a) ONU block diagram of user u.
b) Example of an RSC-encoder, $R_c = 1/2$ and $M_1 = 2$, $G_{1,r} = 07$ and $G_1 = 05$. ($\bigoplus$ is mod-2 addition)

and is given by

$$L = 1/R_c \, . \tag{1}$$

The discrete-time index m after spreading is interrelated to k by $m(k,i) = Lk + i$, $i = 0, \ldots, L-1$. The coded bits are scrambled by a random interleaver. Interleaving is necessary for enhancing iterative MU-detection as will become clear later. Finally, the scrambled sequence of coded bits is fed to a Mach-Zehnder modulator which is responsible for the mapping, impulse shaping and modulation of the light wave signal provided by the laser diode (PD). The output of the modulator is the continuous-time light wave signal $s_u(t)$.
Recently, advanced modulation formats like amplitude- and/or phase-shift-keying techniques have been investigated for its use in optical transmission. Owing to those promising approaches, we employ optical quadrature amplitude modulation (OQ^{2}AM)[5] for mapping. This modulation format includes in addition to the temporal symbol components (I and Q), known from QAM-modulation in the electrical domain, another 2 spacial ones which refer to orthogonal polarization directions. In this paper we focussed on simple binary antipodal OQ^{2}AM exploiting only one direction of polarization. This is also known as BPSK. The bits of the scrambled bit sequence $s_{u,m} \in \{0,1\}$ are then mapped to the four-dimensional symbols $((+1,0)(0,0))$ or $((-1,0)(0,0))$ where the inner pairs of brackets separate the directions of polarization. For ease of notation, we use already the mapped values ± 1 for the scrambled sequence $s_{u,m}$ and neglect the unused dimensions. Nevertheless, the proposed MU-detection scheme also works properly for other or even higher order OQ^{2}AM constellations.

Fig. 2 b) shows an example for an RSC-encoder in order to introduce a compact notation for the different convolutional codes which have been investigated for application as signature codes in OCDMA. Branch $i \in \{1, \ldots, L-1\}$ of the encoder may be characterized by the 3-tupel $(M_i, G_{i,r}, G_i)$ with M_i being the number of delay elements. It is convenient to use octal representation for the feedback polynomial $G_{i,r}$ and the feedforward polynomial G_i. We always assign to 3 consecutive coefficients $r_{i,l} \in \{0,1\}$ of $G_{i,r}$ and $g_{i,l} \in \{0,1\}$ of G_i (weights for the output of the delay elements), $l \in 0, \ldots, M_i$, one octal number by identifying the output weights of the rightmost delay element (r_{i,M_i} and g_{i,M_i}) as least significant bit position of the corresponding binary decomposition. The systematic branch is always labelled by '0', whose specification is therefore omitted. As an example, we indicated the coefficients of an RSC code with $R_c = 1/2$ and $(M_1, G_{r,1}, G_1) = (2, 07, 05)$ in Fig. 2 b).

2.2. Multiple Access Channel (Fiber)

The superposition of the different user signals $s_u(t)$, $u = 1, \ldots, U$, on the multiple access (MA) channel is depicted in Fig. 3. If we have a more abstract view on this scenario, exempt from pure physical considerations of superposition of signals, the MA-channel can be considered to be a mapper which groups the different user symbols $s_{1,m}, \ldots, s_{U,m}$ at time instance m to form a common MU-symbol z_m by simple addition. This mapping can be expressed by

$$z_m = \sum_{i=1}^{U} s_{i,m} \, . \tag{2}$$

Since grouping followed by a mapping is nothing but a code which adds no redundancy, the whole transmission scenario can be interpreted as a concatenation of one outer convolutional code of rate $R_{c,tot} = \sum_{i=1}^{U} R_{c,i}$, which

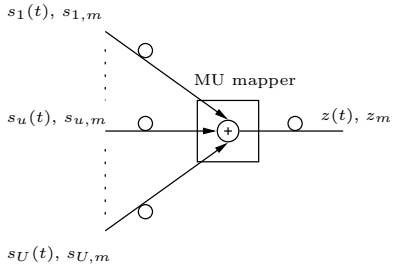

Figure 3. Multiple access fiber acting as additional mapper.

consists of the independant codes of the users, and an inner mapping refering to the superposition of the different user signals. According to this interpretation, the use of iterative decoding algorithms for MU-detection becomes self-evident. Similar to iterative decoding of turbo-codes, actually known from channel coding, we may use 2 stages of decoders/detectors to separate the user information at the receiver while computational complexity is kept within reasonable bounds. Another reason for turbo-like iterative processing at the receiver is the ambiguity which might be introduced by the MA-channel. This will occur anyway if some users map their data by identical OQ^2AM constellations. E.g. 2 users mapping their data to the symbols $+1$ or -1 produces the MU-symbols $z_m \in \{+2, -2, 0\}$ where we do not know without additional information which user has transmitted the positive and which the negative symbol when $z_m = 0$ was received (additional noise neglected). Thus the iterative detector has to provide a-priori information about the symbol each user has transmitted in this worst case scenario.

2.3. Iterative Multiuser Receiver

The interpretation of the multiple access scenario as a code concatenation, which consists of an outer convolutional code and the mapping introduced by the MA-channel, leads to the iterative receiver structure depicted in Fig. 4. The matched filter $g^*(-t)$ includes optical-electrical (O/E) conversion. Since we use OQ^2AM modulation, coherent demodulation with detection of the electrical field strength is required. As a consequence, the additive noise (AWGN) introduced by the detection process remains Gaussian. This is important concering the MU-detection algorithm for which the knowlege about channel statistics is indispensable. After filtering and O/E conversion, the received signal is sampled at a rate of $1/T_c$ in order to recover the MU-symbols z_m which are affected by the additive noise. Hence, we write $\tilde{z}_m$.
The actual MU-receiver consists of 2 soft-in/soft-out (SISO) decoder stages for which we use the superscripts $^{(1)}$ and $^{(2)}$. Thus log-likelihood ratios (L-values) representing soft-bits are passed between the 2 stages. The first one represents a SISO MU-demapper which separates the received $\tilde{z}_m$ into the most likely single user symbols $s_{i,m}$. Those single user symbols are further demapped into its corresponding bit sequence. As already explained above, the a-priori information $L^{(1)}_{A,u}$ is crucial in this case since identical OQ^2AM constellations of the users might lead to ambiguous MU-symbols z_m. After MU-demapping and deinterleaving the users' soft-bits are passed to the outer single user SISO decoders. This decoder stage exploits the code constraints imposed by convolutional encoding at the transmitter and leads to updated a-priori knowlegde of the coded bits $c_{i,m}$ which is fed back to

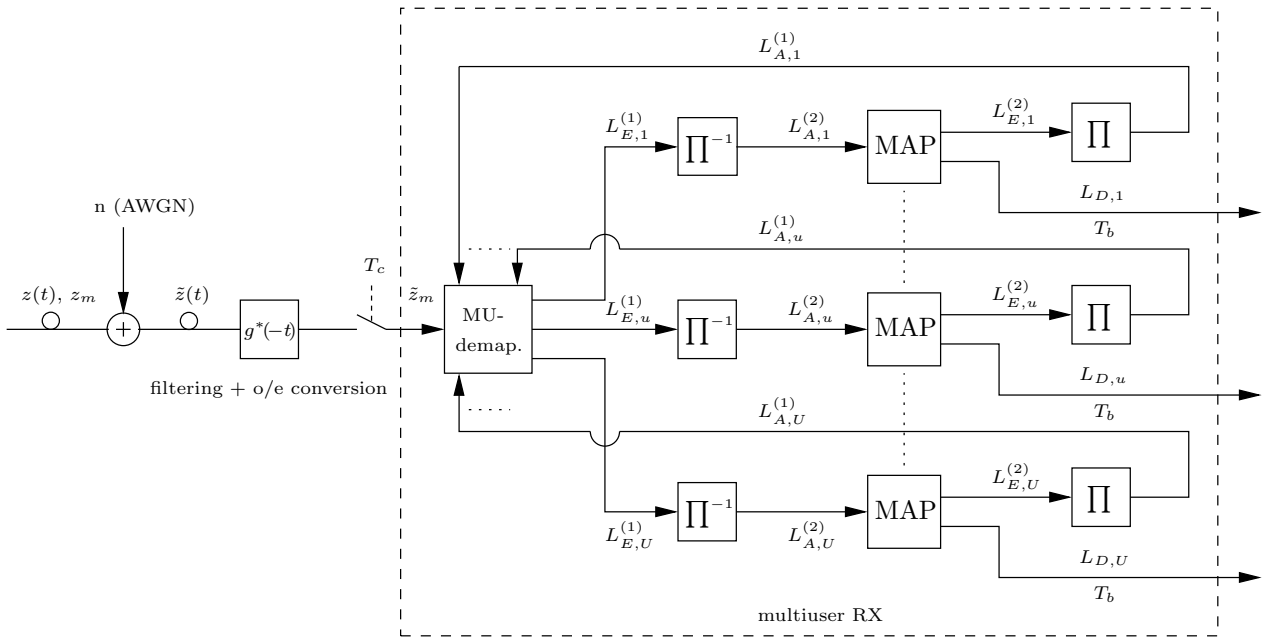

Figure 4. Iterative structure of multuser receiver.

the MU-demapper.
The following Section 3 will give insight in the necessary mathematical operations at the 2 decoder stages.

3. ITERATIVE MULTIUSER DETECTION

3.1. MU-Demapper

The iterative MU-receiver resembles much to iterative demapping and decoding of binary coded modulation (BICM) which has already been invesitgated.[7] The computational complexity of the iterative demapping depends there exponentially on the number of coded bits which are grouped for mapping to one common constellation symbol. In a multiuser scenario, the MA-channel groups the symbols $s_{i,m}$, $i = 1, \ldots, U$, of the users to form the common MU-symbol z_m (cf. (2)). Hence, the same algorithm[7] applied to MU-demapping would have in general a complexity which goes exponentially with the number of constellation symbols if we assumed the same for all users. The number of constellation points of a single user itself depends exponentially on the number of grouped bits. Thus we would arrive at a double exponential complexity on the bit level if we used iterative demapping and decoding.[7] Consequently, we have to employ other strategies to reduce complexity for multiuser demapping.

For the derivation and initial performance evaluation of the iterative procedure of MU-detection we neglect impulse shaping and set $g(t) = \delta(t)$ which leads to an equivalent discrete-time represenation of the system. Assume that we are interested in demapping $\tilde{z}_m$ with respect to user u. By means of eq. (2) we can write for the transmitted symbol of user u

$$s_{u,m} = z_m - \sum_{\substack{i=1 \\ i \neq u}}^{U} s_{i,m} \ . \tag{3}$$

According to eq. (3), we can recover $s_{u,m}$ from the received $\tilde{z}_m$ if we are able to subtract the interference stemming from the other users. This interference can be estimated by exploiting the a-priori information provided by the single user MAP-decoders. An a-priori L-value[8] for the antipodal OQ^{2}AM symbol $s_{i,m}$, $i \neq u$, is defined as

$$L_{A,i}^{(1)}(s_{i,m}) = \ln \frac{P[s_{i,m} = +1]}{P[s_{i,m} = -1]} \tag{4}$$

where the unused dimensions have been skipped for simple notation. Since $P[s_{i,m} = +1] + P[s_{i,m} = -1] = 1$, the a-priori L-values $L_{A,i}^{(1)}(s_{i,m})$ can be retransformed to the respective probabilities

$$P[s_{i,m} = \pm 1] = \frac{\exp(\frac{\pm L_{A,i}^{(1)}(s_{i,m})}{2})}{\exp(\frac{L_{A,u}^{(1)}(s_{i,m})}{2}) + \exp(-\frac{L_{A,i}^{(1)}(s_{i,m})}{2})} \ . \tag{5}$$

These probabilities are used to determine an expectation $\overline{s}_{i,m}$ for the transmitted user symbols

$$\begin{aligned} E[s_{i,m}] \quad = \quad \overline{s}_{i,m} \quad &= \quad (+1) \cdot P[s_{i,m} = +1] + (-1) \cdot P[s_{i,m} = -1] \\ &\overset{(5)}{=} \quad \tanh\left(\frac{L_{A,u}^{(1)}(s_{i,m})}{2}\right) \ . \end{aligned} \tag{6}$$

The total expected interference may now be subtracted from the received MU-symbols $\tilde{z}_m$ to obtain the desired symbol of user u

$$\tilde{s}_{u,m} = \tilde{z}_m - \sum_{\substack{i=1 \\ i \neq u}}^{U} \overline{s}_{i,m} \ . \tag{7}$$

Finally, the extrinsic and channel L-value[8] can easily be computed by

$$L_{E,u}^{(1)}(s_{u,m}) = \ln \frac{p(\tilde{s}_{u,m} | s_{u,m} = +1)}{p(\tilde{s}_{u,m} | s_{u,m} = -1)} \tag{8}$$

with

$$p(\tilde{s}_{u,m}|s_{u,m}=\pm 1)=\frac{1}{\sqrt{2\pi}\sigma_n}\exp\left(-\frac{(\tilde{s}_{u,m}\mp 1)^2}{2\sigma_n^2}\right) \tag{9}$$

being the probability distribution of the AWGN with spectral density $N_0=2\sigma_n^2$ conditioned on the transmitted symbols $s_{u,m}=\pm 1$. After deinterleaving $L_{E,u}^{(1)}(s_{u,m})$ serves as updated a-priori input to the single user MAP-decoder of user u representing the coded bits $c_{u,m}$.

In the very first pass of decoding there is no a-priori information available yet. In this case $P[s_{i,m}=\pm 1]=1/2$. Consequently, $\tilde{s}_{u,m}=\tilde{z}_m$ and we are not able to remove any MU-interference. If, after several iterations, we get reliable a-priori information by the single user MAP-decoders, MU-interference will be completely removed and $\tilde{s}_{u,m}$ will only be affected by AWGN.

It is obvious that calculating the expected MU-interference has a complexity which is only growing linearly with increasing number of users. Furthermore, it is even possible to extend this approach for higher order single user constellations whose symbols depend on more than one bit.

3.2. Single User MAP-Decoder

After MU-demapping and deinterleaving the extrinsic L-values calculated by eq. (8) are passed as new a-priori information $L_{A,u}^{(2)}(c_{u,m})$ to the single user MAP-decoders which apply the well-known BCJR[6]-Algorithm in the log-domain (also known as log-MAP-Algorithm) tailored to iterative decoding. The splitting into U single user MAP-decoders is another advantage of this iterative receiver and the decoding of the convolutional code is performed in parallel for each user.
In the iterative mode the single user MAP-decoders provide updated soft-information $L_{E,u}^{(2)}(c_{u,m})$ on the coded bits $c_{u,m}$ (cf. also transmitter structure). After interleaving, the $L_{E,u}^{(2)}(c_{u,m})$ become again the input a-priori information $L_{A,u}^{(1)}(s_{u,m})$ to the MU-demapper. At this point, it is obvious that interleaving may enhance system performance since correlation among adjacent extrinsic L-values is removed. The processing loop is repeated by steadily increasing the knowlege of MU-interference in terms of $L_{E,u}^{(2)}(c_{u,m})$ and $L_{A,u}^{(1)}(s_{u,m})$, respectively. Thus the estimates on the transmitted symbols calculated for each user by the MU-demapper become more and more reliable.
For final decoding the MAP-decoder determines the a-posteriori L-values $L_{D,u}(b_{u,k})$ for the information bits $b_{u,k}$ which correspond most likely (in a-posteriori sense) to the received equivalent of the coded bit sequence $(c_{u,m_1},\ldots,c_{u,m_2+(L-1)})$, $m_1\leq m(k)\geq m_2$ processed jointly by the decoder in terms of forward and backward recursion of the BCJR-Algorithm. The estimate $\hat{b}_{u,k}$ is made by considering the sign of $L_{D,u}(b_{u,k})$. Good decoding results for $\hat{b}_{u,k}$ will be obtained if the MU-demapper is able to totally remove MU-interference. Then, the MAP-decoder has only to deal with the additive noise distortion in this case and we may end up in single user performance. This holds only for the worst case scenario where all carriers are synchronized. With asynchronous transmission single user performances does not state the ultimate performance bound anymore.

4. PERFORMANCE MEASURES - SIMULATION RESULTS

In this section we study solely the performance of the proposed iterative MU-receiver. Therefore, $g(t)=\delta(t)$ and the fiber is assumed to be an ideal channel. In principle, there are 3 possible parameter sets which can be used to make the superimposed user information distinct from each other:

- RSC code parameters
- interleaver mapping
- single user constellation

We have chosen to use the same RSC codes and the same antipodal OQ^{2}AM constellation for all users whereas the random interleaver mapping is generated by different seed values and is therefore varying. This setup is a special case, i.e. if we further distinguished those parameters, we could arrive at higher system performance.

Nevertheless, the parameters of the user-spanning RSC code are varied in order to find best system performance in terms of minimum required or available bandwidth, convergence of the iterative MU-receiver and bit error ratio (BER). The code memory has been restricted to 4 in order to keep the trellis complexity within reasonable bounds (≤ 16 states). Thus decoding complexity of the MAP-decoders themselves is quite small. The interleaver size is always fixed to 100000 coded bits.

The extrinsic information transfer chart[9] (EXIT-chart) has been proposed as a suitable mean to assess the convergence of iterative receivers with respect to the employed codes by use of the mutual information measure. The crucial point is that we are able to investigate the MU-demapper and single user MAP-decoders independently by varying the input a-priori information and plot the results into one EXIT-chart which allows predictions on the overall decoding performance. We measure in principle the L-value distributions $p(e|x)$ for L_E conditioned on the transmitted bits x with respect to a given a-priori information I_A at the respective demapper/decoder output and determine the mutual information

$$I_E(I_A) = \frac{1}{2}\sum_X \int_{-\infty}^{\infty} p(e|x)\,\mathrm{ld}\frac{2\cdot p(e|x)}{p(e|x=+1)+p(e|x=-1)}de\ . \tag{10}$$

If we refer to the demapper characteristic of user i, the random variable X must be set to S_i and E corresponds to $L_{E,i}^{(1)}$. In the same way, $X = C_i$ and $E = L_{E,i}^{(2)}$ for the decoding characteristic of the respective MAP-decoder. In principle, it is necessary to determine the demapping transfer characteristics of the MU-demapper and MAP-decoder with respect to each single users. Since all users have the same antipodal OQ^{2}AM constellation and the same RSC code, we can rely on one common transfer characteristic for demapper and MAP-decoder, respectively. Thus we set $I_{E1}(I_{A1}) := I_{E_i^{(1)}}(I_{A_i^{(1)}})$ for the demapping transfer characteristic and $I_{E2}(I_{A2}) := I_{E_i^{(2)}}(I_{A_i^{(2)}})$ for the MAP-decoders. The demapping characteristic depends also on the signal-to-noise ratio (SNR) which is defined with respect to one single user

$$\left.\frac{E_b}{N_0}\right|_{dB} = 10\log\frac{E_S\cdot R_c}{N_0} \tag{11}$$

with $N_0 = 2\sigma_n^2$ being the spectral density of the AWGN.
Since I_{E1} becomes I_{A2} and I_{E2} becomes I_{A1}, we can plot $I_{E1}(I_{A1})$ and $I_{E2}(I_{A1})$ into one diagram, called EXIT-chart, by labeling the axis appropriately. The EXIT-chart measurements are carried out by modeling the input a-priori information by a Gaussian distributed random variable which is a convenient assumption.[9]

A last subsection provides simulation results of the BER with respect to E_b/N_0, the number of users and the best matching RSC codes found by EXIT-chart considerations. Those results are compared to coded optical WHC CDMA, i.e. an OCDMA system which has additional error protection by a rate 1/2 RSC code followed by spreading with WHC.

4.1. Convergence Behavior vs. required Code Rate

4.1.1. Initial results

In Fig. 5 the EXIT-chart for a system with 2 and 3 users is depicted with a code rate of 1/2. The transfer characteristic is plotted within the range of $0-10dB$ in steps of $2dB$. The performance of the given system setup is determined by the intersection point and/or the shape of the corridor between the 2 transfer characteristics. If there is no intersection point and a wide corridor, error free transmission will be possible with few iterations. Otherwise, performance gets stuck even when the number of iterations is increased.[9] We found out that the RSC code with $(M_1, G_{r,1}, G_1) = (2, 07, 05)$ provides a good trade-off between early convergence in terms of E_b/N_0 and final performance when the corridor opens up.
As can be seen from Fig. 5 a) and b), the EXIT-chart predicts that we can operate 2 users while it is not possible to allow 3 ones within the specified E_b/N_0-range. If we sketched the decoding trajectory in Fig. 5 b) whose edges should move between the 2 transfer characteristics, it would end right in the intersection point and mutual information between transmitted and decoded information is not very high in this case. The straight lines in Fig. 5 indicate the MU-demapper transfer characteristic for one single user where iterating does not provide a gain in mutual information since no MU-interference exists which may be canceled out. For $I_{A1} = 1$ the transfer characeristics of the MU-demapper ends up in a common point for any given E_b/N_0, i.e. for $I_{A1} = 1$, which can

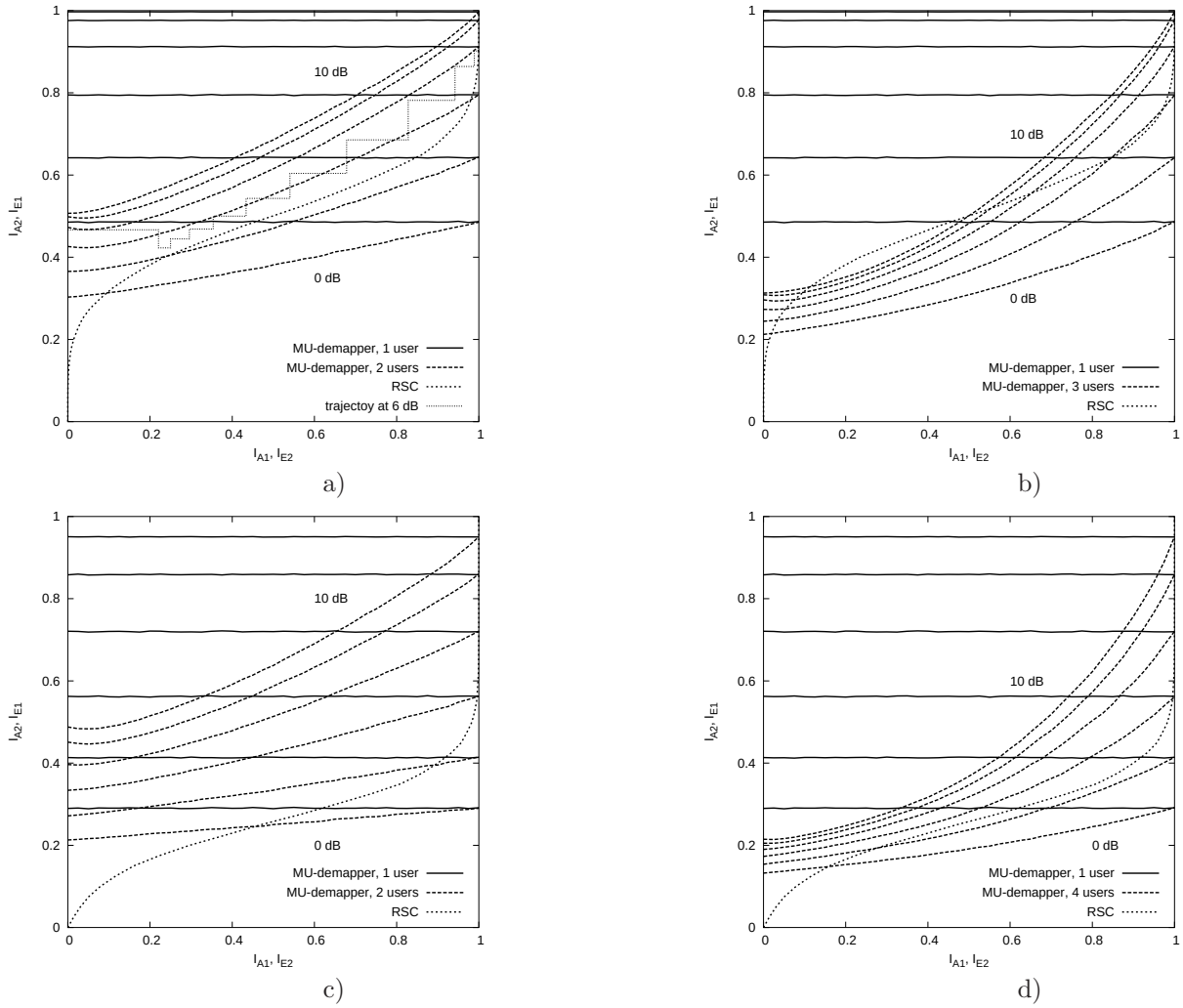

Figure 5. EXIT-chart for $R_c = 1/2$, $(M_1, G_{r,1}, G1) = (2, 07, 05)$: a) 2 users and b) 3 users.
EXIT-chart for $R_c = 1/4$, $(M_1, G_{r,1}, G1) = (0, 00, 01)$, $(M_2, G_{r,2}, G2) = (1, 03, 01)$, $(M_3, G_{r,3}, G3) = (2, 07, 05)$: c) 2 users and d) 4 users.

be possibly reached, we end up in single user performance. Thus, the straight lines of the single user transfer characteristic indicate the ultimate performance bound of the given system setup.
Additionally, we simulated the decoding trajectory for 2 users in Fig. 5 a) at $E_b/N_0 = 6dB$. Unfortunately, it only matches for $I_{A1} = 0$ and $I_{A1} \approx 1$ with the transfer characteristic of the MU-demapper. The edges never reach the transfer characteristic of the RSC code. Accoring to the EXIT-chart, only few iterations should be necessary to reach good performance. Nevertheless, the trajectory includes about 15 iterations, i.e. the EXIT-chart may only provide a rough estimate on the real convergence behavior. The difference between decoding trajectory and transfer characteristics can be explained by the Gaussian assumption of a-priori L-values which is inaccurate and does not take care of MU-interference inherently present in the output of the MU-demapper for small values of I_{A1}.

4.1.2. Decreasing code rate

When we decrease the code rate, convergence behavior improves as can be seen for 2 users in Fig. 5 c). The used RSC code has rate 1/4, $(M_1, G_{r,1}, G_1) = (0, 00, 01)$, $(M_2, G_{r,2}, G_2) = (1, 03, 01)$ and $(M_3, G_{r,3}, G_3) = (2, 07, 05)$. A code rate of 1/4 allows also the operation of 4 users (cf. Fig. 5 d)). From this we can conclude that the

number of supported users increases with decreasing code rate. Of course, efficiency with respect to systems with orthogonal spreading has to be kept in mind when using EXIT-charts for system optimization.

4.2. BER simulations

In Fig. 6 a) - c) the BER of the iterative MU-detection scheme is plotted vs. E_b/N_0 and with respect to different rates of the RSC code. When we compare the results for the different code rates, the predictions of the EXIT-chart considerations have been approved. For a code rate of 1/2 and the best matching RSC code it is hard to reach single user performance even for 8 iterations (cf. Fig. 6 a)). A decrease in code rate allows single user performance for about 4 iterations as depicted in Fig. 6 b) and c).

In Fig. 6 d) we compare convolutionally encoded OCDMA with coded orthogonal WHC OCDMA, i.e. we encode the information bits by a rate 1/2 RSC code and then apply spreading to the coded bits. The total code rate of the system is then 1/4 since the length of the spreading code is minimum 2 if WHC is employed for 2 users. The convolutionally encoded system has a code rate of 1/3 while performance in terms of BER is quite identical with only 4 iterations. This feature of convolutionally encoded OCDMA enhances flexibility of resource management because the available bandwidth may be adjusted according to the actual number of active users.

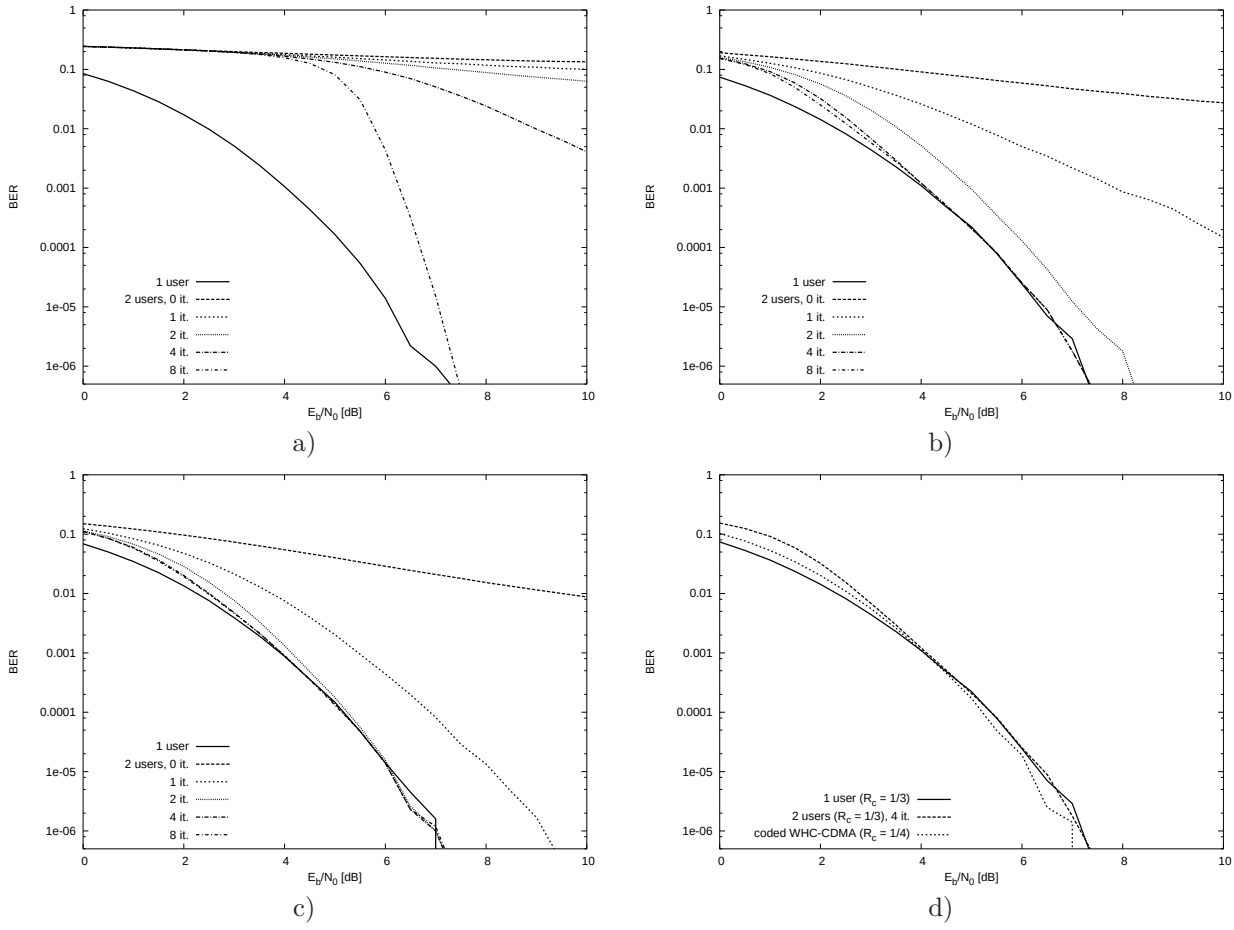

Figure 6. BER-charts for 2 users:
a) $R_c = 1/2$, $(M_1, G_{r,1}, G1) = (2, 07, 05)$
b) $R_c = 1/3$, $(M_1, G_{r,1}, G1) = (1, 03, 01)$ and $(M_2, G_{r,2}, G2) = (2, 07, 05)$
c) $R_c = 1/4$, $(M_1, G_{r,1}, G1) = (0, 00, 01)$, $(M_2, G_{r,2}, G2) = (1, 03, 01)$, $(M_3, G_{r,3}, G3) = (2, 07, 05)$
d) Comparison of convolutionally encoded OCDMA with coded orthogonal WHC OCDMA ($R_c = 1/2$, $(M_1, G_{r,1}, G1) = (2, 07, 05)$)

We observed that the gain of convolutionally encoded OCDMA over WHC CDMA in terms of required code rate increases for increasing number of users, i.e. we may save more coded bits to transmit one information bit of a specific user.

5. SIMULATION RESULTS WITH SSM-FIBER MODEL

Fig. 7 demonstrates the performance of convolutionally encoded OCDMA when a model of a standard single mode fiber (SSMF) is taken into account. The SSMF includes chromatic (CD) as well as polarization mode dispersion (PMD) and length dependent non-linear effects. For impulse shaping a raised cosine filter with roll-off 0.5 is used. This explains why the performance seems to be much better compared to the former results. The chosen fiber lengths are $1km$ and $10km$ and the laser power is set to $1mW$ and $10mW$.
From Fig. 7 a) we can conclude that none of the channel impairments do affect system performance for a fiber length of $1km$. If the fiber length is increased to $10km$, we will observe a slight degradation of performance. The degradation is due to non-linearities. Since in a MU-scenario we cannot neglect this effect, the number of users and, consequently, the overall transmit power may be large.

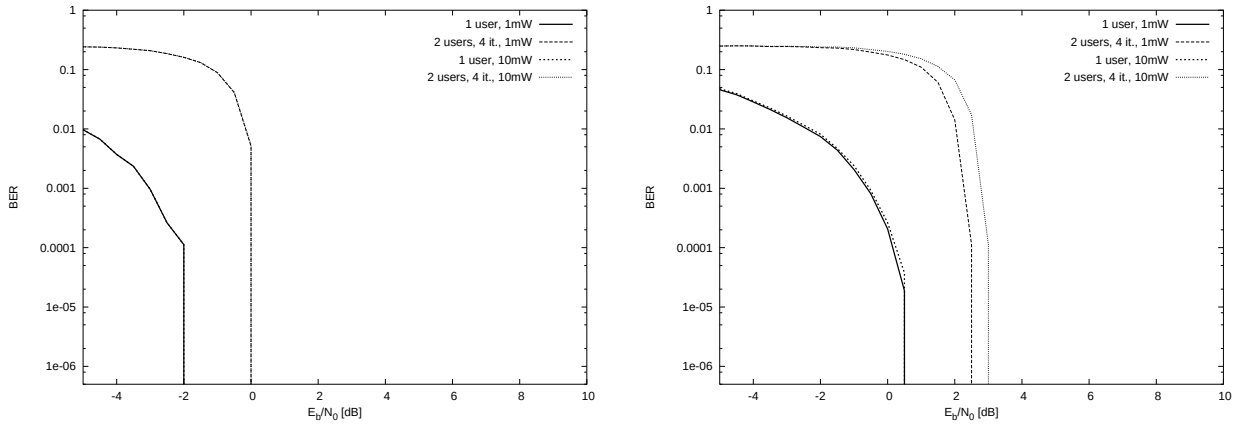

Figure 7. BER (SSMF) for 2 users, $R_c = 1/2$, $(M_1, G_{r,1}, G1) = (2, 07, 05)$: a) $1km$ and b) 10km fiber length.

Apart from the fiber effects, Fig. 7 reveals that filtering may further reduce the required code rate because in Fig. 6 a) single user performance is reached at $E_b/N_0 \approx 7dB$ for rate $1/2$ and 8 iterations. In contrast to this, single user performance is reached here within almost the whole considered range of Fig. 7 and only 4 iterations are necessary.

6. CONCLUSION

We presented an iterative receiver structure for convolutionally encoded OCDMA. The iterative receiver has only linearly increasing complexity in MU-demapping and is applicable to a large amount of users. It was shown that our system proposal, which combines user separation and FEC, is able to outperform those using orthogonal signatures and that it allows greater flexibility in resource management. Further enhancement, especially concering the convergence behavior, may be introduced by differential mapping or more sophisticated single user constellations. It also remains to precise or correct the assumption of Gaussian-distributed a-priori information in a MU-scenario for the MU-demapper and the MAP-decoders in order to improve EXIT-chart predictions. Finally, it would be of great interest to investigate the sensitivity of the whole system, especially the receiver, to asynchronous carriers and quantization effects.

REFERENCES

1. Fan R. K. Chung, Jawad A. Salehi, Victor K. Wei, *"Optical Orthogonal Codes: Design Analysis and Applications,"* IEEE Transactions on Information Theory, vol. 35, no. 3, May 1989
2. Jawad A. Salehi, *"Code Division Multiple-Access Techniques in Optical Fiber Networks - Part I: Fundamental Principles,"* IEEE Transactions on Communications, vol. 37, pp. 824-833, August 1989
3. Jawad A. Salehi, Charles A. Brackett, *"Code Division Multiple-Access Techniques in Optical Fiber Networks - Part II: Systems Performance Analysis,"* IEEE Transactions on Communications, vol. 37, pp. 834-842, August 1989
4. A. J. Viterbi, *"Error Bounds for Convolutional Codes and an Asymptotically Optimum Decoding Algorithm,"* IEEE Transactions on Information Theory, vol. IT-13, pp. 260-269, April 1967
5. Robert Fritsch, *"Viterbi Decoding of a convolutionally encoded OCDMA System,"* 5. ITG-Fachtagung Photonische Netze, Fachhochschule der Deutschen Telekom, Leipzig, Germany, May 2004
6. L. R. Bahl, J. Cocke, F. Jelinek, J. Raviv, *"Optimal decoding of linear codes for minimizing symbol error rate,"* IEEE Transactions on Information Theory, vol. 20, pp. 284-287, March 1974
7. S. ten Brink, J. Speidel, R.-H. Yan, *"Iterative demapping and decoding for multilevel modulation,"* IEEE Global Telecommunications Conference (Globecom) 1998, pp. 579-584, November 1998
8. J. Hagenauer, E. Offer, L. Papke, *"Iterative decoding of binary block and convolutional codes,"* IEEE Transactions on Information Theory, vol. 42, no. 2, pp. 429-445, March 1996
9. S. ten Brink, *"Design of Concatenated Coding Schemes based on Iterative Decoding Convergence,"* PhD-Thesis, University of Stuttgart, Germany, 2002